Monthly Covariability of Amazonian Convective Cloud Properties and Radiative Diurnal Cycle

J. Brant Dodson[1, a)] and Patrick C. Taylor[2, b)]

[1]*NASA Postdoctoral Program, NASA Langley Research Center, 21 Langley Blvd, MS: 420, Hampton, VA, USA.*
[2]*NASA Langley Research Center, 21 Langley Blvd, MS: 420, Hampton, VA, USA.*

[a)]Corresponding author: jason.b.dodson@nasa.gov
[b)]patrick.c.taylor@nasa.gov

Abstract. The diurnal cycle of convective clouds greatly influences the top-of-atmosphere radiative energy balance in convectively active regions of Earth, through both direct presence and the production of anvil and stratiform clouds. CloudSat and CERES data are used to further examine these connections by determining the sensitivity of monthly anomalies in the radiative diurnal cycle to monthly anomalies in multiple cloud variables. During months with positive anomalies in convective frequency, the longwave diurnal cycle is shifted and skewed earlier in the day by the increased longwave cloud forcing during the afternoon from mature deep convective cores and associated anvils. This is consistent with previous studies using reanalysis data to characterize anomalous convective instability. Contrary to this, months with positive anomalies in convective cloud top height (commonly associated with more intense convection) shifts the longwave diurnal cycle later in the day. The contrary results are likely an effect of the inverse relationships between cloud top height and frequency. The albedo diurnal cycle yields inconsistent results when using different cloud variables.

1. INTRODUCTION

Resolving the uncertainties in the top of the atmosphere (TOA) radiative flux imbalance remains a major challenge for climate science. Recent research [e.g. Taylor 2014a] suggests that some of the uncertainty is tied to the ability to realistically represent the radiative diurnal cycle (RDC). The monthly variability in regional RDCs is as large as 7 W m^{-2}, which is 80% of the total interannual variability. In convectively active regions such as the Amazon, where the variability in the RDC is large, the TOA flux diurnal cycle is strongly influenced by the convective diurnal cycle. The influences are produced through both the direct radiative effect of the cloud tops, and indirectly through modification of the convective environment (e.g. upper tropospheric humidity). The linkage between the radiative and convective diurnal cycles is of particular interest because of the ongoing difficulty of representing the convective diurnal cycle in climate models [e.g. Dai 2006].

Previous efforts to address this question involve the use of reanalysis data to characterize the atmospheric state [Taylor 2014b, Dodson and Taylor 2016]. However, the results are sensitive to uncertainties in different reanalyses, limiting the robustness of reanalysis-derived results. One possible alternative to reanalyses is to use satellite observations of convective clouds to characterize the convective environment. CloudSat provides convective cloud observation at high enough frequency to yield robust monthly mean anomalies of convective activity in the Amazon. A main benefit to using CloudSat above other satellites is that it observes both deep convective cores (DCCs) and associated anvil and stratiform clouds. These observations are particularly important for relating convective activity with radiative influence, as the anvils and stratiform clouds provide the majority of the radiative effects from convection.

The goal of this paper is to quantify the relationships between RDC monthly anomalies and cloud variable anomalies, and compare the results with the reanalysis-based results from previous research. In addition to the results, we will specifically answer two questions. First, how sensitive are the cloud-based results to the choice of cloud-based variable? Second, how closely do the cloud-based results correspond with the reanalysis-based results?

2. DATA AND METHODOLOGY

In order to relate the TOA radiative flux with cloud variability, two satellite observation are required. First, Clouds and the Earth's Radiant Energy System CERES (Wielicki et al. 1996) is a collection of identical sensors flown on multiple satellites—Terra, Aqua, and NPP—designed to precisely measure the Earth's radiative energy budget (specifically the broadband shortwave and longwave fluxes). Monthly mean diurnal cycle data are taken from the CERES SYN1deg product (Loeb et al. 2009). The data are available at three hourly time resolution, allowing for a useable representation of the RDC. The radiative variables used to represent the RDC are outgoing longwave radiation (OLR), clear-sky OLR (OLRC), longwave cloud forcing (LWCF), total albedo (α, defined as the ratio of reflected shortwave radiation and insolation), clear-sky albedo (αC), and cloud albedo (αL). The diurnal cycles of these variables in the Amazon (indicated in this paper as $[\text{var}]_{DC}$) are discussed by Dodson and Taylor [2016].

Second, CloudSat (Stephens et al. 2008) is a cloud-observing satellite sharing an orbit with Aqua, which carries a 94 GHz radar to observe vertical profiles of multiple cloud properties. The cloud variables derived from radar measurements are separated into three categories – variables derived from all clouds, variables derived from DCCs only, and variables derived from anvils only. Vertical cloud profiles containing DCCs are identified using three criteria: 1) the cloud must be at least 10 km deep, 2) the cloud must have a maximum reflectivity value of at least 0 dBZ, and 3) the cloud must have a continuous region of reflectivity in the middle troposphere of at least -5 dBZ. Anvil clouds are identified as any cloud connected to a DCC profile with a cloud base above 5 km. The five variables presented here are the occurrence frequency for all clouds (COF), DCCs (DOF), and anvils (AOF); and the cloud top heights for DCCs (DTH) and anvils (ATH).

The comparison methodology is adapted from Taylor [2014b] and Dodson and Taylor [2016]. We regress the diurnal cycle anomalies of individual radiative variables against anomalies in individual cloud variables. In other words, the regression analysis is applied to averages of the radiative variables calculated eight times per day, at 3-hourly intervals, instead of full-daily or full-monthly averages. Anomalies are calculated on the monthly time scale, by subtracting the climatological monthly mean. The analysis is limited to the monthly time scale because of the limited spatial coverage of CloudSat's curtain swath. All monthly anomaly values are represented as [var]′. Relationships between a RDC variable anomaly and a cloud variable anomaly will be written as $[\text{radiation}]_{DC}'/[\text{cloud}]'$.

3. RESULTS

3.1 Cloud Occurrence Frequency

Figure 1a and 1b shows the results for when COF′ is used as the cloud variable. The results for DOF′ and AOF′ (not shown) closely resemble the results for COF′, which reflects the large correlation between the three cloud types (Table 1). For longwave variables, OLR_{DC}'/COF' increases in the morning and decreases in the afternoon during months when COF′ is positive. This is primarily a consequence of the relationship between $LWCF_{DC}'$ and COF′, where $LWCF_{DC}'$ is increased in the afternoon and decreased in the morning (recall the negative sign relationship between the two). However, $LWCF_{DC}'/COF'$ and OLR_{DC}'/COF' are not mirror reflections across the x axis because of the contribution of $OLRC_{DC}'/COF'$. The results in the morning maximum in OLR_{DC}'/COF' occurring three hours before the minimum in $LWCF_{DC}'/COF'$, and the same for the afternoon minimum of the former and maximum of the latter.

TABLE 1. The correlations of the cloud variable monthly anomalies. Statistically significant values ($p \leq 0.01$) are bolded and italicized. All insignificant correlations have $p > 0.1$.

Cloud Variable	COF′	DOF′	AOF′	DTH′	ATH′
Vs. COF′	***1.00***	-	-	-	-
Vs. DOF′	***0.77***	***1.00***	-	-	-
Vs. AOF′	***0.74***	***0.77***	***1.00***	-	-
Vs. DTH′	-0.06	-0.12	-0.09	***1.00***	-
Vs. ATH′	-0.06	0.02	-0.02	***0.49***	***1.00***

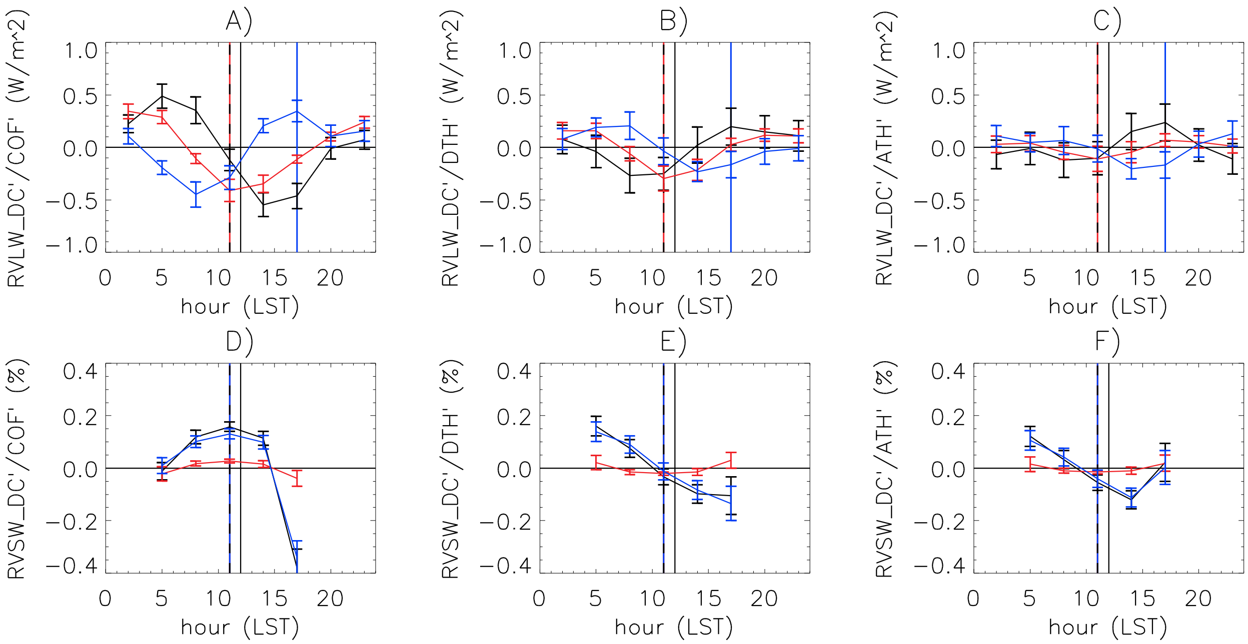

FIGURE 1. The 3-hourly diurnal variability in the $[\text{radiation}]_{DC}'/[\text{cloud}]'$ regression slopes, normalized by the standard deviation of the cloud variables. Longwave and albedo results are shown for COF′ (a,d), DTH′ (b,d), and ATH′ (c,f). $OLR_{DC}'/[\text{cloud}]'$ and $\alpha_{DC}'/[\text{cloud}]'$ shown in black, $OLRC_{DC}'/[\text{cloud}]$ and $\alpha C_{DC}'/[\text{cloud}]'$ in red, and $LWCF_{DC}'/[\text{cloud}]'$ and $\alpha L_{DC}'/[\text{cloud}]'$ in blue. Vertical lines represent the diurnal time of maximum (minimum) for radiative variables (with their respective colors).

These results can be physically interpreted as follows: when the convective environment produces more frequent convection, the increased $LWCF_{DC}$ in the afternoon, resulting from larger areal coverage of anvils and stratiform clouds, shifts OLR_{DC} earlier in the day, and increases the asymmetry in the mean curve about midday. This effect is modulated by the decrease in $OLRC_{DC}$ during midday, which acts to reduce the amplitude of OLR_{DC}, but does not strongly affect the timing. These results and this explanation are similar to those presented by Dodson and Taylor [2016] regarding the relationship of longwave radiation variability to CAPE′, RH250′, and FTS′. This suggests that both the reanalysis-derived results and the CloudSat-derived results are sensitive to the same physical processes that govern convective activity.

The shortwave results (Fig. 1b) show that α_{DC}'/COF' increases midday when monthly COF′ is positive, and greatly decreases in late afternoon. The relationship is almost entirely controlled by $\alpha L_{DC}'/COF'$, and $\alpha C_{DC}'/COF'$ has a mostly negligible contribution. This occurs because the main source of αC, the surface albedo, changes little over the course of the day. The solar zenith angle mostly controls the diurnal cycle of αC, which has negligible monthly perturbations.

This result is difficult to interpret physically. It does not resemble the results for using reanalysis variables (e.g. CAPE′, RH250′) to represent the convective environment. The reanalysis-based results show α_{DC}' increasing in the afternoon when the convective environment is highly unstable, indicating the higher albedo from increased cloud cover (See Dodson and Taylor [2016] for more discussion). The disagreement in cloud-based and reanalysis-based results is likely not an artifact of the limited sampling of CloudSat either, as the reanalysis-based results do not change when the data are constrained to the CloudSat overpass times. The only significant resemblance between the cloud- and reanalysis-based variables occurs in the late afternoon, when the latter also show large decreases in α_{DC}'. This downturn is amplified for dry season-only results (i.e. June-July-August), and is absent for wet season-only results (December-January-February) (not shown), suggesting a connection between late afternoon α_{DC}' and the formation of mesoscale convective systems, which are larger and much more common in the wet season than the dry season [Machado et al. 1998].

3.2 Cloud Top Height

Figure 1e, 1f show the results for DTH′. OLR_{DC}'/DTH' resembles OLR_{DC}'/COF' reflected over the x axis, with one-third of the amplitude. Both $OLRC_{DC}'/DTH'$ and $LWCF_{DC}'/DTH'$ contribute to OLR_{DC}'/DTH' in the same manner as their frequency counterparts do to OLR_{DC}'/COF'. The shortwave results do not resemble α_{DC}'/COF' or the mirrored variant. Instead, α_{DC}'/DTH' decreases steadily throughout the day (less in late afternoon). This resembles the mirrored results for $\alpha_{DC}'/CAPE'$ found by Taylor [2014]. This is closer to the result we may expect to see for α_{DC}'/COF', and is consistent with the physical explanation for $\alpha_{DC}'/CAPE'$ given previously. Further analysis is necessary to determine why the expected relationship occurs more strongly with cloud top height than frequency.

Figure 1g, 1h show the results for ATH′. OLR_{DC}'/CTH' resembles OLR_{DC}'/DTH', except with a smaller amplitude. α_{DC}'/ATH' resembles α_{DC}'/DTH' in that there is a steady decrease through most of the day but also has an increase in the late afternoon, consistent with α_{DC}'/COF' when accounting for the negative correlation between COF′ and ATH′.

The DTH′- and ATH′-based results oppose the frequency-based results, and is related to (small) negative correlations between cloud top height and convective frequency. These results suggest that care must be taken when using cloud variables to represent convective activity. Using different convective variables can yield different results for any analysis of convective behavior or processes.

4. CONCLUSIONS

In this paper, we have quantified the relationships in monthly anomalies between multiple cloud variables and the RDC. These results show that the answers to the questions posed in Section 1 are:

1) The relationships between the RDC and cloud anomalies are highly dependent on the choice of cloud variable, to the point that different variables can yield the opposite results. This does not indicate that cloud variables are useless for representing convective activity, but rather highlights the need for future research to carefully consider the interrelationships between different cloud variables.

2) Cloud frequency-based relationships correspond most closely with reanalysis-derived convective instability-based relationships for the longwave portion of the RDC. Cloud top height-based results show weaker opposing relationships to the frequency-based results, which is consistent with the negative correlations between the variables. The shortwave portion of the RDC has less correspondence between the cloud-based and instability-based results, for reasons that will be determined in future research.

ACKNOWLEDGMENTS

This work has been supported by NASA grant # NNH13ZDA001N-TERAQ, “The Science of Terra and Aqua”, and by the NASA Postdoctoral Program, administered by Universities Space Research Association under contract with NASA.

REFERENCES

Dai, A., “Precipitation Characteristics in Eighteen Coupled Climate Models,” J. Climate **19**, 4605–4630 (2006).

Dodson, J. B., and P. C. Taylor, “Sensitivity of Amazonian TOA flux diurnal cycle composite monthly variability to choice of reanalysis,” J. Geophys. Res. Atmos. **121**, 4404–4428 (2016).

Loeb, N. G., B. A. Wielicki, D. R. Doelling, G. L. Smith, D. F. Keyes, S. Kato, N. Manalo-Smith, and T. Wong, “Toward optimal closure of the earth’s top-of-atmosphere radiation budget,” J. Clim. **22**, 748-766 (2009).

Machado, L. A. T., W. B. Rossow, R. L. Guedes, and A. W. Walker, “Life Cycle Variations of Mesoscale Convective Systems over the Americas,” Mon. Wea. Rev. **126**, 1630-1624 (1998).

Stephens, G. L. and coauthors, “CloudSat mission: Performance and early science after the first year of operation,” J. Geophys. Res. **113**, D00A18 (2008).

Taylor, P. C., “Variability of monthly diurnal cycle composites of TOA radiative fluxes in the tropics,” J. Atmos. Sci. **71**, 754–776 (2014a).

Taylor, P. C., “Variability of Regional TOA Flux Diurnal Cycle Composites at the Monthly Time Scale,” J. Atmos. Sci. **71**, 3484-3498 (2014b).

Wielicki, B. A., B. R. Barkstrom, E. F. Harrison, R. B. Lee III, G. L. Smith, and J. E. Cooper, “Clouds and the Earth’s Radiant Energy System (CERES): An Earth observing system experiment,” Bull. Amer. Meteor. Soc. **77**, 853-868 (1996).